UNIVERSITY OF LEEDS

This is a repository copy of *Raman optical activity of human α -synuclein in intrinsically disordered, micelle-bound α -helical, molten globule and oligomeric β -sheet state*.

White Rose Research Online URL for this paper:
http://eprints.whiterose.ac.uk/118620/

Version: Accepted Version

Article:
Mensch, C, Konijnenberg, A, Van Elzen, R et al. (3 more authors) (2017) Raman optical activity of human α -synuclein in intrinsically disordered, micelle-bound α -helical, molten globule and oligomeric β -sheet state. Journal of Raman Spectroscopy, 48 (7). pp. 910-918. ISSN 0377-0486

https://doi.org/10.1002/jrs.5149

© © 2017 John Wiley & Sons, Ltd. This is the peer reviewed version of the following article: Mensch, C., Konijnenberg, A., Van Elzen, R., Lambeir, A.-M., Sobott, F., and Johannessen, C. (2017) Raman optical activity of human α-synuclein in intrinsically disordered, micelle-bound α-helical, molten globule and oligomeric β-sheet state. J. Raman Spectrosc., doi: 10.1002/jrs.5149.; which has been published in final form at https://doi.org/10.1002/jrs.5149. This article may be used for non-commercial purposes in accordance with the Wiley Terms and Conditions for Self-Archiving.

Reuse
Items deposited in White Rose Research Online are protected by copyright, with all rights reserved unless indicated otherwise. They may be downloaded and/or printed for private study, or other acts as permitted by national copyright laws. The publisher or other rights holders may allow further reproduction and re-use of the full text version. This is indicated by the licence information on the White Rose Research Online record for the item.

Takedown
If you consider content in White Rose Research Online to be in breach of UK law, please notify us by emailing eprints@whiterose.ac.uk including the URL of the record and the reason for the withdrawal request.

White Rose university consortium
Universities of Leeds, Sheffield & York

eprints@whiterose.ac.uk
https://eprints.whiterose.ac.uk/

Raman optical activity of human α-synuclein in intrinsically disordered, micelle-bound α-helical, molten globule and oligomeric β-sheet state.

Carl Mensch[a,b], Albert Konijnenberg[c], Roos Van Elzen[d], Anne-Marie Lambeir[d], Frank Sobott[c,e], Christian Johannessen[a*]

[*]Correspondence to: Prof. Dr. Christian Johannessen, University of Antwerp, Groenenborgerlaan 171, B-2020 Antwerp, Belgium. E-mail: Christian.Johannessen@uantwerpen.be

[a]Molecular Spectroscopy Group, Department of Chemistry, University of Antwerp, Antwerp, Belgium.

[b]Ghent Quantum Chemistry Group, Department of Inorganic and Physical Chemistry, University of Ghent, Ghent, Belgium.

[c]Biomolecular and Analytical Mass Spectrometry, Department of Chemistry, University of Antwerp, Antwerp, Belgium.

[d]Laboratory of Medical Biochemistry, Department of Pharmaceutical Sciences,
University of Antwerp, Antwerp, Belgium.

[e]Astbury Centre for Structural Molecular Biology, University of Leeds, Leeds, UK.
School of Molecular and Cellular Biology, University of Leeds, Leeds, UK.

Abstract

α-synuclein (α-syn) is a 140 residue protein that plays a central role in Parkinson's disease (PD) and other neurological disorders. The precise function and pathological properties of α-syn remain however poorly understood. While α-syn is considered to be a flexible and disordered protein under native conditions, its ability to adopt a variety of conformational ensembles depending on the environment is considered to be related to its pathology. Raman optical activity (ROA) is a chiroptical spectroscopic technique that is uniquely sensitive to the secondary structure of proteins in solution and was used here for the first time to study the different conformational ensembles of α-syn. In this paper, the Raman and ROA spectral characteristics of these different conformations of α-syn are investigated. We show that Raman and ROA spectroscopy are sensitive enough to not only detect transitions from a disordered to an α-helical or a β-sheet rich ensemble, but also to differentiate between the α-helical forms of wild-type (WT) and C-terminal truncated α-syn 107. Using increasing concentrations of fluorinated alcohols we induce the aggregation pathway of α-syn and identify a molten globule intermediate structure and β-sheet rich oligomers. Taken together, these results demonstrate the power of Raman and ROA spectroscopies for the structural elucidation of proteins that are challenging to characterise.

Keywords

Raman optical activity, protein structure, Parkinson's disease, spectral sensitivity.

Introduction

α-synuclein (α-syn) is a protein that is abundantly expressed in the brain, where it is mainly located in the presynaptic terminals and the nucleus.[1,2] Although its physiological function remains unknown,

α-syn has been suggested to be involved in the regulation of presynaptic vesicles, neurotransmitter release, synaptic function and neuronal plasticity.[3–8] It plays a central role in the pathogenesis of Parkinson's disease (PD), dementia with Lewy bodies (DLB) and multiple system atrophy (MSA). These neurodegenerative diseases are often referred to as (α-)synucleinopathies, since intracellular proteinaceous inclusions mainly consist of fibrillar aggregates of α-syn.[9–11] This was reported for the first time in 1997 when Spillantini *et al.* showed that Lewy Bodies and Lewy neurites, the pathological hallmarks of PD and DLB, contain α-syn.[11] Missense mutations (A53T, A53E, A30P, E46K, G51D, H50Q) and gene duplications or triplications of *SNCA*, the gene that encodes for α-syn, are linked to familial PD.[12–19] Furthermore, sequence variation in *SNCA* has been identified by genome-wide associations studies to be an important risk factor for idiopathic PD.[20] After Alzheimer's disease, DLB is considered the second most common neurodegenerative disease, which explains the vast amount of research that focusses on α-syn to elucidate both its native and pathologic properties.[21] Nevertheless, the precise mechanism and pathologic properties of this protein are still unknown.[22]

A key aspect of elucidating the etiology of PD and related neuropathies, is the characterisation of the structural propensities of α-syn. Such structural insight can provide insight in the disease progression and could aid in the development of therapeutics.[22,23] Although the native structure of α-syn has been the matter of debate in scientific literature, a recent study using in-cell nuclear magnetic resonance (NMR) and electronic paramagnetic resonance (EPR) showed α-syn to be a monomeric and intrinsically disordered protein (IDP) in mammalian cells.[24] While this native structure is very dynamic, α-syn adopts a predominantly α-helical structure upon interaction with lipid membranes and detergent micelles (see ***Figure 1***).[25] Both this membrane bound α-helical form as well as partial α-helical structure have been proposed to play a role in the pathologic process and aggregation of α-syn.[26,27] Nevertheless, the fibrillary aggregates, the pathological hallmarks of DLB, contain a high content of β-sheet structure.[28] Because of its ability to adopt different structures and conformations depending on the environment, α-syn has been called a chameleon protein.[29] Depending on the environment, α-syn has been observed in α-helical, β-sheet, partially folded and disordered conformations, besides appearing in monomeric, oligomeric and aggregated forms.[30]

In this study, Raman optical activity (ROA) is employed to characterise the different conformational propensities of α-syn as this spectroscopic technique is exceptionally sensitive to protein secondary structure in solution, giving spectral patterns not only specific to each type of secondary structure, but sensitive to small alterations and fine-structure details of the conformation.[31–33] This case study serves to demonstrate the power of Raman and ROA to study proteins that are challenging to characterise, such as α-syn. Structural biology is a multidisciplinary field combining both experimental and computational techniques and ROA might provide complementary structural information due to its unique sensitivity to the secondary structure of proteins.

Here, we report the Raman and ROA spectroscopic characteristics of solution phase α-syn adopting disordered (IDP), α-helical, partially folded and β-structure conformations. The different conformational states of α-syn have been studied and reported in scientific literature based on multiple techniques such as NMR, small-angle X-ray scattering (SAXS) and circular dichroism (CD) and α-syn is thus an ideal protein to explore the structural sensitivity of ROA in this case study. In aqueous solutions, α-syn is an IDP, which was for example demonstrated previously by Syme *et al.* using ROA.[34] In the presence of negatively charged lipids, the N-terminal region (Asp2-Thr92) folds into an amphipathic α-helix through the KTKEGV consensus sequence, similar to apolipoproteins.[8,35]

Inspired by the NMR study by Ulmer *et al.*, the α-helical structure of α-syn interacting with sodium dodecyl sulphate (SDS) micelles used as membrane mimics, is studied here for the first time based on ROA.[36] Since recent work by our group demonstrated that ROA is very sensitive to subtle changes in α-helical conformations,[33] also the structure of the A30P mutant of α-syn (α-syn A30P) in the presence of SDS micelles was studied using ROA. This missense mutation replaces an alanine by a proline and disrupts a minor part of the α-helical structure α-syn adopts on the micelle surface (see *Figure* ***1***).[37] The acidic and proline-rich C-terminal region of α-syn remains disordered in these α-helical structures of α-syn. For that reason, also the Raman and ROA spectra of a C-terminally truncated variant of α-syn are reported here to evaluate the sensitivity of ROA to both α-helical and disordered structure. Although α-helical intermediates have been reported to be involved in the aggregation pathway of α-syn, the fibrillary aggregates of α-syn predominantly contain β-sheet structure.[28] The central portion of the α-syn sequence (Glu61-Val95, called the non-amyloid component or NAC domain[38]) has a high propensity for β-sheet structure and was shown to drive amyloid formation.[39,40] Since ROA is commonly measured from isotropic solutions it is not feasible to obtain the ROA spectra of fibrillated forms of α-syn. However, small (fluorinated) alcohols such as 2,2,2-trifluoroethanol (TFE) have been reported in scientific literature to induce β-structure alongside other structures of α-syn, depending on the concentration of TFE.[41,42] At low concentrations of TFE (< 10 % v/v) partially folded intermediates are observed, at intermediate concentrations of TFE (10-35 % v/v), α-syn aggregation is induced, while at high concentration of TFE (> 35 % v/v) α-helical structure is detected.[41,42] Although at higher concentration of TFE ROA measurements were not feasible due to a high turbidity of the solution possibly because of aggregation of α -syn, the Raman and ROA patterns of α-syn in 5 % and 10 % v/v TFE are reported and discussed here. The spectral characteristics and differences among the various conformations of α-syn are discussed in detail as this study of α-syn is a valuable example of the potential of ROA for structural biology.

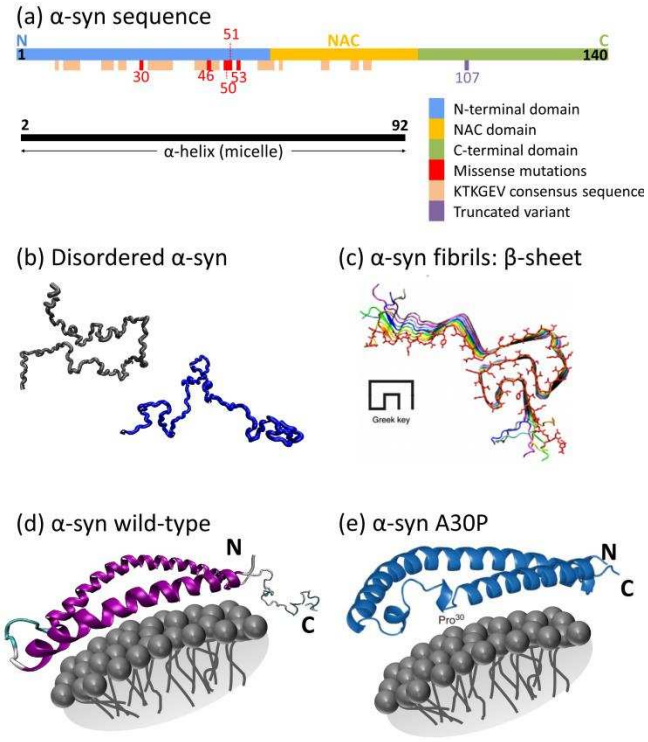

Figure 1 Sequence and structure of α-syn: (a) Sequence of full length α-syn (residues 1-140) with indication of the three domains (N-terminus 1-60, non-amyloid beta component (NAC; 61-95) and C-terminus 96-140), missense mutations (A53T, A53E, A30P, E46K, G51D, H50Q), the KTKEGV motive and the residues that adopt α-helical secondary structure upon interaction with SDS micelles (residues 2-92). (b) Two conformers of the NMR-based ensemble of intrinsically disordered α-syn reported by Schwalbe et al.[43] *(c) Representation of the cross-β sheet structure adapted from Tuttle et al.*[44] *(d) WT α-syn adopting an α-helical structure upon interaction with SDS micelles (PDB id. 1XQ8)*[36] *compared to (e) the average secondary structure of the A30P variant of α-syn without displaying the disordered C-terminus, adapted from Ulmer and Bax.*[37] *VMD version 1.9.2 was used to represent the α-syn structures as cartoons in (b) and (d). In (d) and (e) a partial SDS micelle is represented in grey, merely for illustrative purposes.*

Materials and Methods

Chemicals

All chemicals were purchased at Sigma-Aldrich with purities > 99.0 % unless stated otherwise.

Expression and purification of human α-syn (WT, α-syn 107)

Recombinant wild-type (WT) and truncated (1-107) human α-syn protein were produced in *E.coli* BL21(DE3) cells using the pT7-7 expression system and purified with minor modifications as described elsewhere.[45] For the truncated form, a stop codon was inserted after bp 321 of the cDNA of human WT α-syn via site-directed mutagenesis (QuickChangeII, Agilent). Summarized, the cells were harvested 5 hours after IPTG (1 mM; Thermo Scientific, Erembodegem, Belgium) induction, resuspended in 10 mM Tris-HCl pH 8, 1 mM EDTA supplemented with complete Protease inhibitor cocktail (Roche Diagnostics, Vilvoorde, Belgium), heat denatured (6°C 45 min), and lysed by sonication followed by centrifugation (10.000 x g 20 min at 4°C). A serially executed streptomycin sulphate precipitation (1% m/v centrifuged at 13.500 x g for 30 min at 4 °C) and ammonium sulphate precipitation (30% m/v centrifuged at 13.500 x g for 30 min at 4 °C) were carried out on the clarified supernatant. The resultant semi-pure WT α-syn 107 pellets were resuspended in 10 mM Tris-HCl pH

7.4 or pH 8 resp. and loaded on HiPrep 16/60 Sephacryl S-100 HR column (GE Healthcare, Machelen Belgium) using an Åkta chromatography system (GE Healthcare). Next, WT α -syn fractions were pooled and anion exchanged (HiLoad 16/10 Q sepharose HP column, GE Healthcare), while α-syn 107 was purified by sequential anion exchange (1 ml HiTrap Q, GE Healthcare) and cation exchange (1 ml HiTrap SP, GE Healthcare). In both cases fractions of highly pure α-syn were collected upon generation of linear gradient towards buffer B (10 mM Tris-HCl pH 7.4 and pH 8 resp, 0.5 M NaCl). α-syn containing fractions were pooled and dialyzed against 50 mM ammonium bicarbonate, lyophilized and stored until use at -80°C. The purity and concentration of the proteins was determined using SDS-PAGE and a Pierce BCA protein assay. Lyophilized α-syn A30P was kindly donated by prof. R. Grandori (University of Milano-Bicocca) and used without further purification.

Sample preparation for Raman and ROA spectroscopy

Protein solutions for Raman and ROA spectroscopy were prepared by dissolving the lyophilised protein (WT α-syn, α-syn 107, α-syn A30P) in deionised water, aqueous SDS solution (Amersham Biosciences, 99.0%, Uppsala, Sweden; stock solution with a concentration of SDS of 328 mM) or TFE (5% or 10% v/v in deionised water) to a final concentration of 30-50 mg/mL of protein. The resulting solution was directly loaded in a quartz cuvette and used for Raman and ROA collection.

Raman and ROA spectroscopy

The Raman and ROA spectra were measured at ambient conditions using the previously described ChiralRAMAN-2X scattered circular polarization (SCP) ROA instrument (BioTools, Inc).[46,47] The Raman spectra are displayed as the circular intensity sums ($I_R + I_L$) and the ROA spectra as the circular intensity differences ($I_R - I_L$) with I_R and I_L denoting the scattered Raman intensities with right- and left-circular polarization, respectively. The instrument excitation wavelength was 532 nm; laser power at the source was in the range of 400-800 mW, depending on the sample; spectral resolution of 7 cm^{-1}; and illumination times of 24-40 hours. Solvent spectra were subtracted from the Raman spectra after which the baseline correction procedure by Boelens *et al.* was applied, unless stated otherwise.[48] The ROA spectra were smoothed using a 3rd order, 5-point Savitzky-Golay filter, except when specified otherwise.

Results and Discussion

intrinsically disordered α-synuclein.

The Raman and ROA spectrum of α-syn in aqueous solution show distinct patterns for a protein that is structurally disordered (Figure 2).[34] In the Raman spectrum, the amide I region (1630-1700 cm^{-1}) is the most distinctive spectral region to study secondary structure, as it arises mainly from the carbonyl stretch in the polyamide backbone of the protein. The broad band with a maximum at 1674 cm^{-1} is assigned to disordered structure similar to an earlier report on the Raman characteristics of α-syn in aqueous buffer solution.[49] Although many Raman bands arise from the side-chains of the protein, the extended amide III region (1230-1340 cm^{-1}) is also very sensitive to secondary structure, since it involves in-phase combination of N-H in-plane deformation with C-N stretching.[50] The coupling of N-H and Cα-H deformations in these vibrational modes is very sensitive to the exact geometry. The broad amide III Raman band around 1254 cm^{-1} is assigned to disordered or random protein conformations. While the secondary structure analysis from Raman spectra is hampered by

the many contributions from the side-chains, the strength of ROA stems from its sensitivity to chirality. The main ROA patterns of proteins arise from the most rigid and chiral structural components, which is the peptide backbone conformation; *i.e.* the secondary structure. Most spectral contributions from side-chains cancel out, due to their flexibility and the occurrence of multiple of the same residues with different side-chain conformations. As a result, ROA spectral patterns mainly occur in the amide I, amide III and skeletal stretch (Cα-C, Cα- Cβ and Cα-N stretch; 870-1150 cm^{-1})[31] regions, which makes ROA exceptionally sensitive to secondary structure. However, side-chain CH_2 and CH_3 deformations (1430-1470 cm^{-1})[31,50] and a conformationally sensitive tryptophan band (~ 1550 cm^{-1})[51,52] are separately observed in ROA spectra, for example. The ROA spectrum of α-syn was published before by Syme *et al.* at a lower resolution than the one shown in *Figure 2*. Because of the disordered nature, it seems more challenging to obtain a good signal-to-noise ratio for IDPs. A broad ROA amide I band with a maximum at 1680 cm^{-1} is observed, which is assigned to disordered or polyproline II (PPII; backbone torsion angles ϕ; Ψ of -75°; 145°) structure.[31,33] Based on spectroscopic methods such as ROA, PPII was identified in the past to be an important local conformation of IDPs.[53–55] Model peptides such as the XAO peptide (Ac-XXA_7OO-NH_2) were shown by a multitude of techniques to adopt a flexible structure with torsion angles fluctuating in the PPII region of the Ramachandran plot.[33,54,56] Such structures do not support regular patterns of intramolecular hydrogen bonding. Furthermore, in the amide III region of the ROA spectrum, α-syn shows a maximum at 1324 cm^{-1} which is indicative for this kind of PPII structure implicated in IDPs. This observation confirms that α-syn has many torsion angles found in the PPII region of the Ramachandran plot (fluctuating around -75°;145°). The broadness of the 1324 cm^{-1} band likely stems from structural heterogeneity and solvation of the structure. A -/+ couplet in the skeletal stretch region, negative at 1093 cm^{-1} and positive at 1129 cm^{-1} is observed both for α-helical proteins and IDPs.[33,34] For α-syn, it suggests local residual structure of the backbone, hence either α-helical or PPII-like. Besides the latter couplet, the skeletal stretch region does not show spectral patterns, indicating a flexible and disordered structure. These observations are consistent with structural studies using NMR, which show that *in vitro* α-syn adopts a disordered structure with a large proportion of the backbone torsion angles fluctuating around the ideal angles for PPII structure.[43,57] Also in mammalian cells, α-syn was primarily found as a disordered monomer, however adopting more compact conformations, compared to buffered solution.[24]

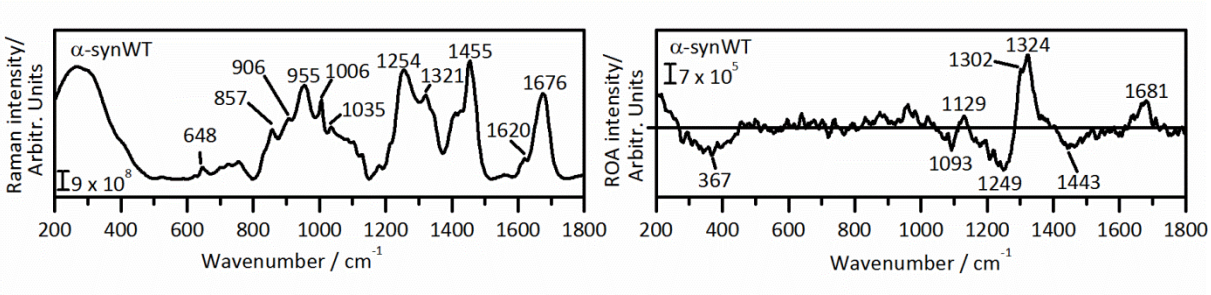

Figure 2 Raman (left; I_R+I_L) and ROA (right; I_R-I_L) of 40 mg/mL human WT α-syn in aqueous solution. The ROA spectrum was baselined by overly smoothing the ROA spectrum using a Savitzky-Golay filter.

α-helical α-synuclein

When α-syn is presented with a membrane mimicking environment, such as SDS micelles, a drastic change to the Raman and specifically the ROA spectrum is observed (*Figure **3***). Compared to the

Raman spectrum of disordered α-syn in aqueous solution (*Figure 2*), a redshift of the amide I band to 1654 cm^{-1} is observed, characteristic of α-helical structure. The intensity of the Raman band observed in disordered α-syn at 1254 cm^{-1} is significantly lower in the SDS solution. The structural difference between disordered α-syn in aqueous solution and α-helical α-syn in SDS solution is distinctly clear in the different ROA spectra. All spectral patterns have changed: The amide I couplet negative at 1627 cm^{-1} and positive at 1667 cm^{-1}, the amide III -/+/+ pattern at 1242/1305/1346 cm^{-1} with the two positive ROA bands characteristic of α-helical structure, a -/+ couplet at 1091/1127 cm^{-1} and positive intensity in the skeletal stretch region at 931 cm^{-1} are all ROA patterns traditionally assigned to α-helical structure.[31,33] This is in accordance with several other reports using CD, SAXS, NMR and EPR of α-syn interacting with SDS or sodium lauroyl sarcosinate (SLAS).[36,58,59] Upon interaction with SDS or SLAS micelles, the N-terminal region of α-syn (residues Asp2-Thr92) adopts an amphipathic α-helix on top of the detergent micelles. The C-terminus remains a disordered tail extending flexibly into solution, as can be seen in the molecular structures deposited in the protein data bank (PDB id. 2KKW[59] and 1XQ8[36]). As shown in the NMR study by Ulmer *et al.,* the structure of micelle-bound α-syn consists of two curved, anti-parallel α-helices (Val3-Val37 and Lys45-Thr92) which are connected by an extended linker of seven residues (Leu38-Thr44) with a propensity to form a turn (see *Figure 1*).[36] The extended amide III region observed here is very similar to the ROA patterns of several viral coat proteins of filamentous bacteriophages (e.g. M13 and fd) that have amphipathic α-helical structures as reported by Blanch *et al*.[60,61] While two positive bands, the first around 1300 cm^{-1} and the second around 1345 cm^{-1}, are observed for α-helical proteins, the intensity ratio of these two bands has been the matter of debate in scientific literature.[32,33,60,62] Based on recent work by our group , the dominant ROA band around 1345 cm^{-1} of α-helical α-syn is assigned to regular α-helical structure,[33] which is consistent with the NMR structure of micelle-bound α-syn (PDB id. 1XQ8). The ROA band observed around 1300 cm^{-1} was shown in our earlier work to be much more sensitive to the conformation of the α-helix than the 1345 cm^{-1} signature. A very intense band at 1300 cm^{-1} indicates either solvent exposure or structural heterogeneity of the helical portions of the protein.[33] The amide III pattern observed here is in accordance with the formation of an amphipathic helix consisting of long stretches of α-helix with a hydrophobic side and a hydrophilic face exposed to the solvent, such as is seen in the NMR structure.

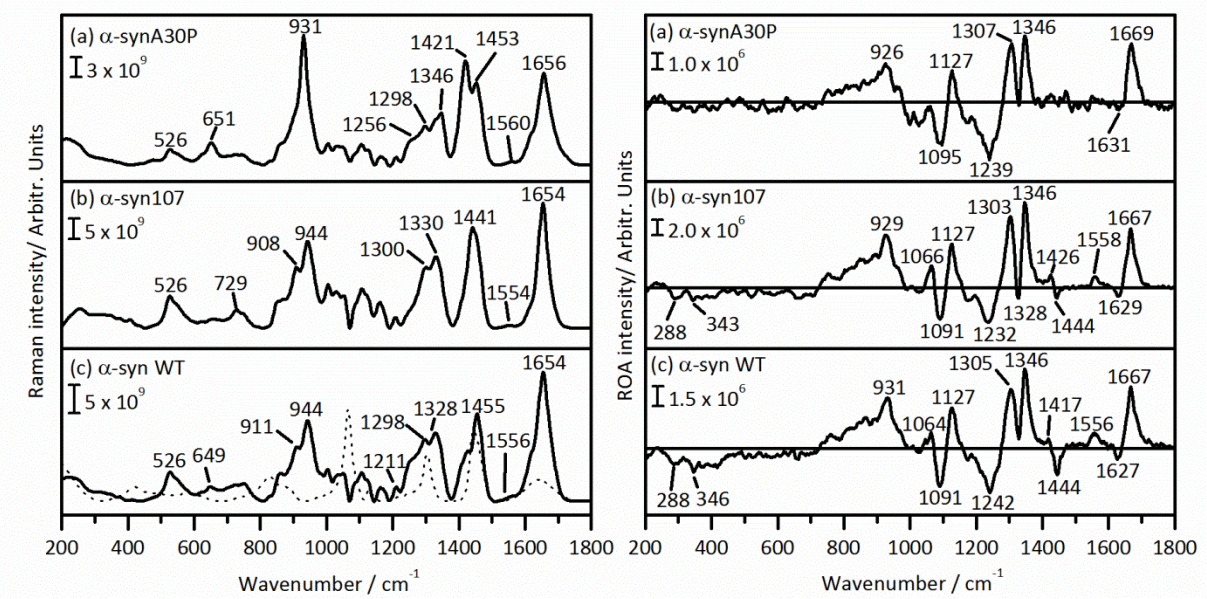

Figure 3 Raman (left; I_R+I_L) and ROA (right; I_R-I_L) spectra of α-syn (50 mg/mL) in a high concentration of SDS (328 mM; 40 times the CMC in water): (a) the α-syn A30P variant; (b) α-syn 107 and (c) WT α-syn. For each Raman spectrum, the Raman spectrum of the SDS solution was firstly subtracted after which the baseline correction by Boelens et al. was applied.[48] *The Raman spectrum of the aqueous SDS solution is given as a dotted line in the panel of the Raman spectrum of WT α-syn.*

Interestingly, while α-syn does not contain a tryptophan residue, which has a distinct band around 1555 cm^{-1}, both the Raman and ROA spectrum of α-syn in SDS solution show a small contribution in the amide II region, clearly identifiable, as SDS also does not have a Raman band in that region. Amide II vibrations arise from out-of-phase N-H in-plane deformations with C-N stretching and are not often distinctly observed in ROA spectra. McColl *et al.* suggested that a positive amide II band might be assigned to β-sheet structure and that unusually large positive amide II bands are a characteristic of flat β-sheet.[63] The ROA spectra of α-helical α-syn however show that such a positive band can also be observed for α-helical structure. It is possible that the local environment of the amides is affected by the interaction of the amphipathic helical structure with the SDS micelles, giving rise to the observed amide II band.

The ROA spectrum of WT α-syn bound to SDS micelles does not contain a significant contribution from the disordered tail. The most prominent amide III band at 1324 cm^{-1} observed in the spectrum of disordered α-syn is not visible in the amide III region of α-helical α-syn. The amide I is a -/+ couplet characteristic for α-helical structure. To investigate whether the disordered tail affects the α-helical N-terminus, and furthermore if a spectral pattern can be deducted for the disordered C-terminus, the ROA spectrum of C-terminally truncated α-syn 107 was recorded. This α-syn form lacks 33 residues from the disordered tail, while the sequence making up the amphipathic α-helix is retained. As can be seen in *Figure 3*, the spectrum of α-helical WT α-syn is very similar to that of the truncated variant. However, it seems small differences in the ROA spectra can be carefully deduced. The amide I region in the ROA spectra of the WT and α-syn 107 is the same, while the amide III region shows minor differences. This demonstrates that the amide III region is the most sensitive to the three-dimensional structure of proteins in solution. Principally, by subtracting the ROA spectrum of α-syn 107 from the WT α-syn spectrum, only the spectrum of the disordered tail is retained, assuming the structure of the α-helical part is unaltered. Since this involves only 33 out of 140 residues, the difference as displayed in *Figure 4* is noisy. Nevertheless, the difference ROA band at 1326 cm^{-1} indicates a higher content of disordered structure in WT α-syn than in C-terminally truncated α-syn 107. The negative features at 1300 cm^{-1} and 1346 cm^{-1} suggest that α-syn 107 adopts a slightly higher α-helical content. However, at this signal-to-noise ratio, care must be exerted not to overly interpret the data. By taking the difference of the Raman spectra, the most prominent positive amide bands are observed at 1251 cm^{-1} (amide III) and 1679 cm^{-1} (amide I), reinforcing the conclusion from the ROA spectra that WT α-syn displays a more disordered structure upon interacting with SDS micelles, since its C-terminus is disordered. The positive band at 1618 cm^{-1} in the Raman difference is observed as five out of five phenylalanine residues and three out of four tyrosine residues occur in the C-terminal sequence, which is not present in the truncated α-syn 107 variant. The small negative contribution at 1652 cm^{-1} also suggests α-syn 107 adopts a slightly higher α-helical content. The spectral differences in the regions 1000-1140 cm^{-1} and 1430-1460 cm^{-1} are difficult to interpret as the corresponding vibrational modes comprise CH_2 and CH_3 deformations both of the protein and SDS (1064 cm^{-1} and 1459 cm^{-1}).

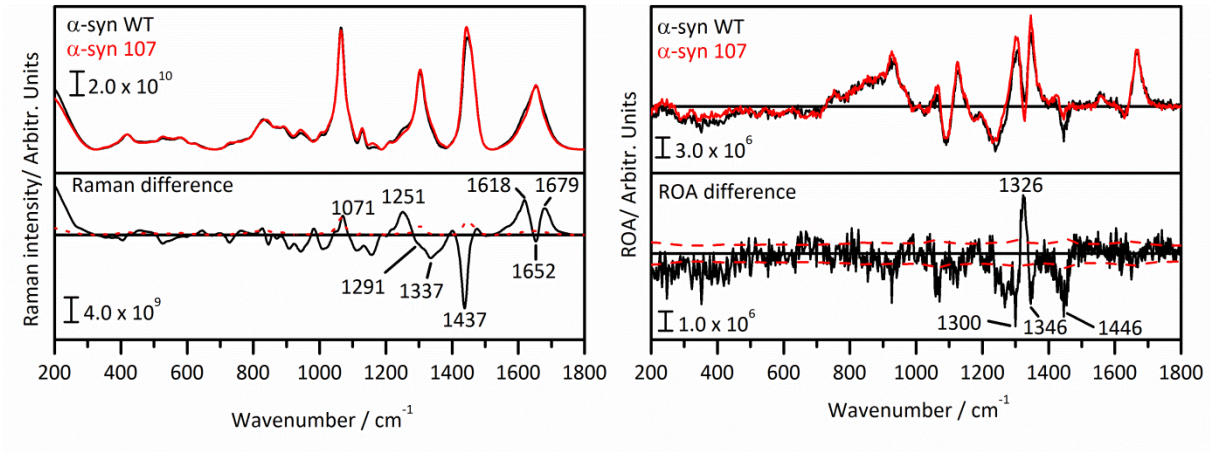

Figure 4 Raman (left; I_R+I_L) and ROA (right; I_R-I_L) spectral differences of WT α-syn (black solid line) and α-syn 107 (red solid line): The top panels present the aligned spectra with their respective difference (α-syn 107 subtracted from WT α-syn) shown in the bottom panels. The square root of the WT α-syn Raman spectrum multiplied by 2 and -2 is plotted as the dashed red lines in the bottom right panel. These lines represent an estimation of the shot noise level (multiplied by 2 due to the difference of 2 spectra). The Raman spectra were firstly baselined before the subtraction.[48] The Raman spectrum of the SDS solution was not subtracted, but it is shown on top of the Raman difference spectrum as a red dashed line to represent regions where SDS has intense Raman bands. The ROA spectra of WT α-syn and α-syn 107 and the difference are the raw measured data without smoothing or baseline correction.

A number of hereditary missense mutations have been identified that are related to the aggregation propensity of α-syn and developing of early onset of synucleinopathies. Although some mutations (eg. A53T) do not directly influence the ensemble structure of α-syn monomers interacting with micelles, the A30P mutation , which due to the introduction of a proline residue interrupts one helix turn (Val26-Ala29), causes the N-terminal α-helix to terminate at Ala27 instead of Val37.[37] The A30P mutation has been shown to disrupt the equilibrium between the membrane bound and cytosolic α-syn species and might explain the early onset of synucleinopathies observed for patients with this missense mutation.[64,65] The NMR study by Ulmer and Bax revealed that the backbone order changes for approximately 10 residues in the micelle-bound A30P mutant compared to WT α-syn, while the remainder of the structure essentially remains unaffected. [37] The ROA spectrum of the A30P mutant of α-syn shows a very similar pattern compared to the WT. The effect of a change in the short stretch of α-helix that changes to an extended disordered conformation is not evidently visible in the spectrum. This is in accordance with the results discussed above, that mainly the most chiral parts of the protein are picked up by ROA. Furthermore, a change in secondary structure in 10 amino acids (7 % of the protein) is a subtle change compare to a truncation of 33 residues (24 % of the protein). Although disordered structure has a characteristic ROA pattern, the spectrum here is dominated by signals arising from the predominantly α-helical structure that is stable. Even so, the ROA spectrum of A30P in the presence of SDS micelles does appear to contain slight differences from WT α-syn, which ideally should be studied in more detail. Unfortunately, it was not possible to produce a difference spectrum of sufficient quality to detect the minor spectral differences that could be expected with the small change in secondary structure caused by the A30P mutation (see Figure S.1). Based on the strong sensitivity of the ROA band around 1307 cm^{-1} to small conformational changes, a larger change of the band intensity would be expected concomitant with a change in the helicity or flexibility.[33] This is in accordance with the NMR study by Ulmer and Bax that showed that the backbone order only changed significantly for the residues Gln24–Lys32; the N-terminal α-helix did not reveal a significant change.[37] The only significant spectral change in the difference ROA

spectrum shown in Figure S.1, is a negative ROA band with a minimum at 1446 cm^{-1}, which is present in the ROA spectrum of WT α-syn and not in that of the A30P variant. This spectral difference likely supports the slightly different interaction of the protein with the micelle and concomitant effect on the micelle shape reported by Ulmer and Bax.[37] The spectral region around 1446 cm^{-1} arises from CH_2 and CH_3 deformations, hence a change in the interaction of the protein with SDS micelles could alter the spectral contribution from the aliphatic chains of the detergent. Nevertheless, the small structural changes induced by the A30P mutation are apparently enough to induce defective membrane binding for the A30P mutant.

α-synuclein forms a partially folded state and oligomerizes in low concentrations of TFE.

Considering the involvement of α-syn in PD and related neurodegenerative diseases, one of the most studied aspect of this protein is its aggregation properties.[27,41,42,58,66,67] The use of small, fluorinated alcohols has been proposed in the past to model the effect of phospholipid vesicles on α-syn.[41,42] Although 2,2,2-trifluoroethanol (TFE) is often used in structural biology to induce α-helical structure, when α-syn is incubated in intermediate concentrations of TFE (10-20 % v/v) it forms β-sheet-rich fibrillary species.[41,42] At concentrations above 40 % v/v of TFE, highly α-helical α-syn is observed. Unfortunately, at such high concentration of TFE, we were not able to record ROA because of too low solubility and hence high turbidity of the sample because of the high protein concentration required for ROA measurements. Nonetheless, the Raman and ROA spectra of α-syn in aqueous solution with 5 % v/v or 10 % v/v TFE were recorded and are depicted in *Figure 5*. The amide I region of both Raman spectra displays a maximum at 1669-1671 cm^{-1}, which together with the amide III band around 1241-1246 cm^{-1} indicates β-sheet structure both at 5 % and 10 % v/v TFE, mixed with disordered structure. Compared to the ROA spectra of α-syn in its IDP and α-helical states, the ROA spectra in TFE solution are distinctly different, again illustrating the secondary structure sensitivity of ROA. Different ROA spectra for proteins containing diverse forms of β-sheet have been reported, however, as reviewed by Weymuth and Reiher, only a few signatures can be regarded as reliable β-sheet characteristics while many other β-sheet and turn signatures have been suggested.[68] They propose that only a -/+ couplet centred around 1650-1670 cm^{-1} and negative intensity in the region 1240-1255 cm^{-1} are reliable markers of β-sheet structure. Yet, positive intensity in the extended amide III region 1260-1330 cm^{-1}, flanked by negative intensity on both sides 1240-1255 cm^{-1} and 1240-1280 cm^{-1} is consistently observed for proteins containing mainly β-sheet structure.[31,63] Overlap or proximity of characteristic regions of different secondary structure types together with the large diversity of β-structure impedes the detailed assignment of marker bands of β-sheet, which complicates a detailed analysis of the ROA patterns observed here. In the spectrum of α-syn in 10 % TFE, the -/+ couplet, negative at 1662 cm^{-1} and positive at 1678 cm^{-1} is indicative of β-sheet. However, in 5 % TFE the negative contribution of the amide I couplet is not present. This observation suggests that in 10 % TFE the content of β-sheet is higher, while in 5 % TFE there are contributions of a mixture of secondary structure elements. The latter sample remained stable for multiple days during ROA acquisition, while in 10 % TFE the aggregation of α-syn complicated the ROA measurement due to increased light scattering from particulates in the sample, which explains the lower signal-to-noise that could be obtained from this sample. Similar narrow amide I ROA bands such as the one at 1678 cm^{-1} in the 5 % TFE measurement were previously reported for the Bowman-Birk protease inhibitor[55], the A-state of α-lactalbumin[69] and the intermediate states in the renaturing of insulin from its amyloid state[70]. In these reports this band was assigned to a disordered type of conformation with PPII contribution. It should however be noted that in the ROA spectra of proteins

and peptides with a disordered/PPII type of structural propensity, the amide I is considerably broader, arising from a flexible structure surrounded by water. In this case, α-syn in 5 % TFE adopts a more compact structure compared to its intrinsically disordered structure in water. Interestingly, the positive band at 1564 cm^{-1} can be assigned to amide II vibrations since α-syn has no tryptophan residue in its sequence, similar to the assignment of this spectral band of poly-L-lysine in a mainly β-sheet state.[63] The negative band observed at 1617 cm^{-1} in the spectra of α-syn in both 5 % and 10 % TFE and more generally the +/-/+/-/+ pattern at 1564/1617/1637/1662/1678 cm^{-1} in 10 % TFE is reminiscent of this spectral region in the ROA spectra of reduced hen lysozyme,[31] reduced bovine ribonuclease A,[31] reduced prion (PrP^{94-223}),[63] the molten globule A-state of bovine α-lactalbumin[69] and the renaturing intermediate of insulin amyloid[70], which are all dynamic states of these proteins that populate different secondary structure elements. Also a few β-sheet proteins display a similar pattern in the 1540-1700 cm^{-1} region such as P.69 pertactin,[63] of which the crystal structure resembles models of amyloid structure due to its parallel β-sheet arrangement,[71] and poly-L-lysine in a β-sheet state.[63] The latter observations might suggest that such a ROA pattern arises from the formation of β-sheet structure, indicating that oligomeric species are present, which was for example also suggested before for reduced hen lysozyme.[31] This also implicates that α-syn in 10 % TFE forms oligomers, which is reasonable considering the high concentration of α-syn (30 mg/mL) in this sample. In 5 % TFE, the lack of the positive band at 1037 cm^{-1}, no negative intensity around 1340-1380 cm^{-1} and no negative band at 1662 cm^{-1} indicate a more dynamic structure with the population of different secondary structures. These assignments of the ROA patterns are however tentative as the 1540-1700 cm^{-1} comprises the amide II, amide I and aromatic residues (tyrosine and phenylalanine ~ 1600-1625 cm^{-1}; tryptophan ~ 1555 cm^{-1})[50], which might couple to the amide vibrations. The 1561 cm^{-1} band in the ROA spectrum of poly-L-lysine (which lacks aromatic residues), for example, was however assigned to amide II vibrations, since hydrogen/deuterium exchange resulted in a large shift of this band, demonstrating the involvement of N-H protons (the amide II vibration is an in-phase combination of NH in-plane deformation and CN stretching).[63] To conclude the discussion above, ROA indicates that in 5 % TFE α-syn adopts a partially folded structure. Such a state of α-syn has been referred to as a pre-molten globule by Uversky,[30] which is consistent with the high similarity of the ROA spectrum of α-syn in 5 % TFE with that of e.g. the molten globule A-state of α-lactalbumin.[69] In 10 % TFE, α-syn (here at 30 mg/mL) aggregates with the formation of β-sheet rich structures. The ROA spectrum of α-syn in 10 % TFE is very similar to that of reduced ovine PrP^{94-233}, which was suggested by McColl *et al.* to be characteristic of unusually flat and regular β-sheet structure.[63] Both in 5 % and 10 % TFE, α-syn is known to aggregate upon agitation (shaking at 37°C) for a prolonged time.[42] Previously, Anderson *et al.* reported that in 5 % TFE amyloid fibrils were formed, while in 10 % TFE classic amyloid fibrils were not observed but flexible, short “TFE fibrils” were formed.[42] Probably, the ROA spectrum in 5 % represents an intermediate state in the TFE aggregation pathway.

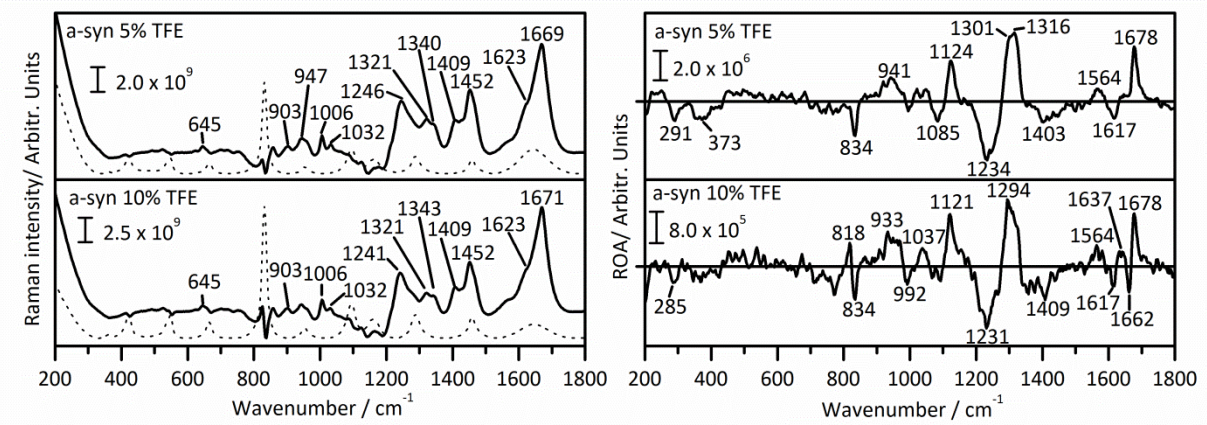

Figure 5 Raman (left; I_R+I_L) and ROA (right; I_R-I_L) spectra of 30 mg/mL α-syn in 5 % (top) and 10 % v/v (bottom) TFE in demineralised water. The baselined[48] Raman spectrum of the corresponding TFE solutions are given in dashed lines in comparison to the Raman spectra of α-syn (solid line) to illustrate which spectral regions (e.g. around 832 cm^{-1} in Raman and ROA) are sensitive to solvent artefacts. Due to scattering from larger particles indicating aggregation of α-syn in 10 % TFE, a lower resolution was obtained in ROA for the corresponding ROA spectrum. Furthermore, because of the higher stability of the 5 % TFE sample, the sample was monitored with Raman and ROA for one week, but did not change over time.

Conclusions

Although the protein α-synuclein (α-syn) plays a central role in Parkinson's disease, both its precise involvement in the pathology as well as its native function are poorly understood. α-syn is challenging to characterise since its structure is very sensitive to its environment; it is capable of adopting disordered, helical, β-sheet and partially folded structures. As this structural behaviour has received much attention in scientific literature, α-syn provided an ideal case study to assess and demonstrate the secondary structure sensitivity of Raman and ROA to characterise the different conformations of α-syn. In the present study, we show that all the main forms of secondary structure elements, e.g. disordered, helical and β-sheet, dominate α-syn under different conditions and can be studied by ROA. In aqueous solution, α-syn is an intrinsically disordered protein, as shown by the Raman and ROA spectra. In the presence of SDS micelles, α-syn adopts a stable α-helical structure. Comparison of the Raman and ROA spectra of WT α-syn with the C-terminally truncated (at residue 107) variant reveals that the C-terminal of the WT variant remains disordered upon interaction with detergent micelles, consistent with reports in literature based on CD and NMR techniques. The truncated variant α-syn 107 seems to have a slightly higher α-helical structure. The A30P mutant of α-syn adopts an α-helical structure upon interaction with detergent micelles comparable to the WT. Although a short stretch of α-helix is lost due to the mutation, the ROA spectra of the A30P mutant and WT α-syn did not reveal a significant difference, thus demonstrating the limit of ROA in detecting structural differences. The α-helical conformation is not significantly altered due to the A30P mutation, nor has its hydration significantly increased. In 5 % v/v TFE, α-syn adopts a pre-molten globule or partially folded structure, which probably is an intermediate in the formation of aggregates. The ROA spectrum is very similar to that of α-syn in 10 % TFE. However, in 10 % TFE a few bands clearly show a higher content of β-structure, indicating oligomerization and aggregation of α-syn. The results are in accordance with earlier reports on the various structures of α-syn based on, for example, NMR and CD and hence demonstrate the use of Raman and ROA to characterise proteins that are of interest in structural biology, both as complementary and stand-alone tools.

Acknowledgements

The authors thank prof. R. Grandori (University of Milano-Bicocca) for the kind donation of the A30P mutant of α-synuclein. Financial support through the BOF-GOA concerted research grant '4D protein structure' is acknowledged. Furthermore, the authors acknowledge the financial support provided by the Flemish Community, the University of Antwerp (BOF-NOI) for the pre-doctoral scholarship of C. M. and the University of Ghent (IOF Advanced TT) for the purchase of the ChiralRAMAN-2X.

Supporting information

Supplementary Information may be found in the online version of this article.

References

[1] R. Jakes, M. G. Spillantini, M. Goedert. *Febs Lett.* **1994** ; *345* , 27.
[2] P. J. Kahle, M. Neumann, L. Ozmen, V. Muller, H. Jacobsen, A. Schindzielorz, M. Okochi, U. Leimer, H. van Der Putten, A. Probst, E. Kremmer, H. A. Kretzschmar, C. Haass. *J. Neurosci.* **2000** ; *20* , 6365.
[3] S.-J. Lee, H. Jeon, K. V. Kandror. *Acta Neurobiol. Exp. (Wars).* **2008** ; *68* , 509.
[4] S. Bellani, V. L. Sousa, G. Ronzitti, F. Valtorta, J. Meldolesi, E. Chieregatti. *Commun. Integr. Biol.* **2010** ; *3* , 106.
[5] D. F. Clayton, J. M. George. *Trends Neurosci.* **1998** ; *21* , 249.
[6] H. A. Lashuel, C. R. Overk, A. Oueslati, E. Masliah. *Nat. Rev. Neurosci.* **2013** ; *14* , 38.
[7] D. F. Clayton, J. M. George. *J. Neurosci. Res.* **1999** ; *58* , 120.
[8] J. M. George, H. Jin, W. S. Woods, D. F. Clayton. *Neuron* **1995** ; *15* , 361.
[9] M. G. Spillantini, M. Goedert. *Ann. N. Y. Acad. Sci.* **2000** ; *920* , 16.
[10] M. Goedert, M. G. Spillantini, K. Del Tredici, H. Braak. *Nat Rev Neurol* **2013** ; *9* , 13.
[11] M. G. Spillantini, M. L. Schmidt, V. M.-Y. Lee, J. Q. Trojanowski, R. Jakes, M. Goedert. *Nature* **1997** ; *388* , 839.
[12] J. J. Zarranz, J. Alegre, J. C. Gómez-Esteban, E. Lezcano, R. Ros, I. Ampuero, L. Vidal, J. Hoenicka, O. Rodriguez, B. Atarés, V. Llorens, E. G. Tortosa, T. del Ser, D. G. Muñoz, J. G. de Yebenes. *Ann. Neurol.* **2004** ; *55* , 164.
[13] S. Appel-Cresswell, C. Vilarino-Guell, M. Encarnacion, H. Sherman, I. Yu, B. Shah, D. Weir, C. Thompson, C. Szu-Tu, J. Trinh, J. O. Aasly, A. Rajput, A. H. Rajput, A. Jon Stoessl, M. J. Farrer. *Mov. Disord.* **2013** ; *28* , 811.
[14] R. Krüger, W. Kuhn, T. Müller, D. Woitalla, M. Graeber, S. Kösel, H. Przuntek, J. T. Epplen, L. Schöls, O. Riess. *Nat. Genet.* **1998** ; *18* , 106.
[15] M.-C. Chartier-Harlin, J. Kachergus, C. Roumier, V. Mouroux, X. Douay, S. Lincoln, C. Levecque, L. Larvor, J. Andrieux, M. Hulihan, N. Waucquier, L. Defebvre, P. Amouyel, M. Farrer, A. Destée. *Lancet (London, England)* **2004** ; *364* , 1167.
[16] A. B. Singleton, M. Farrer, J. Johnson, A. Singleton, S. Hague, J. Kachergus, M. Hulihan, T. Peuralinna, A. Dutra, R. Nussbaum, S. Lincoln, A. Crawley, M. Hanson, D. Maraganore, C. Adler, M. R. Cookson, M. Muenter, M. Baptista, D. Miller, J. Blancato, J. Hardy, K. Gwinn-Hardy. *Science* **2003** ; *302* , 841.
[17] P. Pasanen, L. Myllykangas, M. Siitonen, A. Raunio, S. Kaakkola, J. Lyytinen, P. J. Tienari, M. Pöyhönen, A. Paetau. *Neurobiol. Aging* **2014** ; *35* , 2180.e1.
[18] S. Lesage, M. Anheim, F. Letournel, L. Bousset, A. Honoré, N. Rozas, L. Pieri, K. Madiona, A. Dürr, R. Melki, C. Verny, A. Brice, French Parkinson's Disease Genetics Study Group. *Ann. Neurol.* **2013** ; *73* , 459.
[19] M. H. Polymeropoulos, C. Lavedan, E. Leroy, S. E. Ide, A. Dehejia, A. Dutra, B. Pike, H. Root, J. Rubenstein, R. Boyer, E. S. Stenroos, S. Chandrasekharappa, A. Athanassiadou, T.

Papapetropoulos, W. G. Johnson, A. M. Lazzarini, R. C. Duvoisin, G. Di Iorio, L. I. Golbe, R. L. Nussbaum. *Science* **1997** ; *276* , 2045.
[20] W. Satake, Y. Nakabayashi, I. Mizuta, Y. Hirota, C. Ito, M. Kubo, T. Kawaguchi, T. Tsunoda, M. Watanabe, A. Takeda, H. Tomiyama, K. Nakashima, K. Hasegawa, F. Obata, T. Yoshikawa, H. Kawakami, S. Sakoda, M. Yamamoto, N. Hattori, M. Murata, Y. Nakamura, T. Toda. *Nat. Genet.* **2009** ; *41* , 1303.
[21] R. Savica, B. F. Boeve, G. Logroscino, in *Handbook of Clinical Neurology Vol. 138* , (Eds: C. Rosano, M.A. Ikram, M. Ganguli), Elsevier B.V., Amsterdam, **2016** , pp. 153–158.
[22] W. Peelaerts, V. Baekelandt. *Nat. Struct. Mol. Biol.* **2016** ; *23* , 359.
[23] G. Tóth, S. J. Gardai, W. Zago, C. W. Bertoncini, N. Cremades, S. L. Roy, M. A. Tambe, J.-C. Rochet, C. Galvagnion, G. Skibinski, S. Finkbeiner, M. Bova, K. Regnstrom, S.-S. Chiou, J. Johnston, K. Callaway, J. P. Anderson, M. F. Jobling, A. K. Buell, T. A. Yednock, T. P. J. Knowles, M. Vendruscolo, J. Christodoulou, C. M. Dobson, D. Schenk, L. McConlogue. *PLoS One* **2014** ; *9* , e87133.
[24] F.-X. Theillet, A. Binolfi, B. Bekei, A. Martorana, H. M. Rose, M. Stuiver, S. Verzini, D. Lorenz, M. van Rossum, D. Goldfarb, P. Selenko. *Nature* **2016** ; *530* , 45.
[25] D. Eliezer, E. Kutluay, R. Bussell, G. Browne. *J. Mol. Biol.* **2001** ; *307* , 1061.
[26] D. Ysselstein, M. Joshi, V. Mishra, A. M. Griggs, J. M. Asiago, G. P. McCabe, L. A. Stanciu, C. B. Post, J.-C. Rochet. *Neurobiol. Dis.* **2015** ; *79* , 150.
[27] D. Ghosh, P. K. Singh, S. Sahay, N. N. Jha, R. S. Jacob, S. Sen, A. Kumar, R. Riek, S. K. Maji. *Sci. Rep.* **2015** ; *5* , 9228.
[28] L. C. Serpell, J. Berriman, R. Jakes, M. Goedert, R. A. Crowther. *Proc. Natl. Acad. Sci. U. S. A.* **2000** ; *97* , 4897.
[29] V. N. Uversky. *J. Biomol. Struct. Dyn.* **2003** ; *21* , 211.
[30] V. N. Uversky. *J. Neurochem.* **2007** ; *103* , 17.
[31] L. D. Barron, L. Hecht, E. W. Blanch, A. F. Bell. *Prog. Biophys. Mol. Biol.* **2000** ; *73* , 1.
[32] S. Yamamoto, M. Straka, H. Watarai, P. Bour. *Phys. Chem. Chem. Phys.* **2010** ; *12* , 11021.
[33] C. Mensch, L. D. Barron, C. Johannessen. *Phys. Chem. Chem. Phys.* **2016** ; *18* , 31757.
[34] C. D. Syme, E. W. Blanch, C. Holt, R. Jakes, M. Goedert, L. Hecht, L. D. Barron. *Eur. J. Biochem.* **2002** ; *269* , 148.
[35] J. P. Segrest, H. De Loof, J. G. Dohlman, C. G. Brouillette, G. M. Anantharamaiah. *Proteins Struct. Funct. Genet.* **1990** ; *8* , 103.
[36] T. S. Ulmer, A. Bax, N. B. Cole, R. L. Nussbaum. *J. Biol. Chem.* **2005** ; *280* , 9595.
[37] T. S. Ulmer, A. Bax. *J. Biol. Chem.* **2005** ; *280* , 43179.
[38] K. Uéda, H. Fukushima, E. Masliah, Y. Xia, A. Iwai, M. Yoshimoto, D. A. Otero, J. Kondo, Y. Ihara, T. Saitoh. *Proc. Natl. Acad. Sci. U. S. A.* **1993** ; *90* , 11282.
[39] B. I. Giasson, I. V Murray, J. Q. Trojanowski, V. M. Lee. *J. Biol. Chem.* **2001** ; *276* , 2380.
[40] A. Recchia, P. Debetto, A. Negro, D. Guidolin, S. D. Skaper, P. Giusti. *FASEB J.* **2004** ; *18* , 617.
[41] L. A. Munishkina, C. Phelan, V. N. Uversky, A. L. Fink. *Biochemistry* **2003** ; *42* , 2720.
[42] V. L. Anderson, T. F. Ramlall, C. C. Rospigliosi, W. W. Webb, D. Eliezer. *Proc. Natl. Acad. Sci. U. S. A.* **2010** ; *107* , 18850.
[43] M. Schwalbe, V. Ozenne, S. Bibow, M. Jaremko, L. Jaremko, M. Gajda, M. R. Jensen, J. Biernat, S. Becker, E. Mandelkow, M. Zweckstetter, M. Blackledge. *Structure* **2014** ; *22* , 238.
[44] M. D. Tuttle, G. Comellas, A. J. Nieuwkoop, D. J. Covell, D. A. Berthold, K. D. Kloepper, J. M. Courtney, J. K. Kim, A. M. Barclay, A. Kendall, W. Wan, G. Stubbs, C. D. Schwieters, V. M. Y. Lee, J. M. George, C. M. Rienstra. *Nat. Struct. Mol. Biol.* **2016** ; *23* , 409.
[45] M. E. van Raaij, I. M. J. Segers-Nolten, V. Subramaniam. *Biophys. J.* **2006** ; *91* , L96.
[46] L. D. Barron, F. Zhu, L. Hecht, G. E. Tranter, N. W. Isaacs. *J. Mol. Struct.* **2007** ; *834–836* , 7.
[47] W. Hug, G. Hangartner. *J. Raman Spectrosc.* **1999** ; *30* , 841.
[48] H. F. M. Boelens, R. J. Dijkstra, P. H. C. Eilers, F. Fitzpatrick, J. A. Westerhuis. *J. Chromatogr. A* **2004** ; *1057* , 21.
[49] N. C. Maiti, M. M. Apetri, M. G. Zagorski, P. R. Carey, V. E. Anderson. *J. Am. Chem. Soc.* **2004** ;

126 , 2399.
[50] A. Rygula, K. Majzner, K. M. Marzec, A. Kaczor, M. Pilarczyk, M. Baranska. *J. Raman Spectrosc.* **2013** ; *44* , 1061.
[51] C. R. Jacob, S. Luber, M. Reiher. *ChemPhysChem* **2008** ; *9* , 2177.
[52] E. W. Blanch, L. Hecht, L. A. Day, D. M. Pederson, L. D. Barron. *J. Am. Chem. Soc.* **2001** ; *123* , 4863.
[53] Z. Shi, R. W. Woody, N. R. Kallenbach. *Adv. Protein Chem.* **2002** ; *62* , 163.
[54] A. A. Adzhubei, M. J. E. Sternberg, A. A. Makarov. *J. Mol. Biol.* **2013** ; *425* , 2100.
[55] E. Smyth, C. D. Syme, E. W. Blanch, L. Hecht, M. Vašák, L. D. Barron. *Biopolymers* **2001** ; *58* , 138.
[56] F. Zhu, J. Kapitan, G. E. Tranter, P. D. A. Pudney, N. W. Isaacs, L. Hecht, L. D. Barron. *Proteins Struct. Funct. Bioinforma.* **2007** ; *70* , 823.
[57] J. R. Allison, P. Varnai, C. M. Dobson, M. Vendruscolo. *J. Am. Chem. Soc.* **2009** ; *131* , 18314.
[58] L. Giehm, C. L. P. Oliveira, G. Christiansen, J. S. Pedersen, D. E. Otzen. *J. Mol. Biol.* **2010** ; *401* , 115.
[59] J. N. Rao, C. C. Jao, B. G. Hegde, R. Langen, T. S. Ulmer. *J. Am. Chem. Soc.* **2010** ; *132* , 8657.
[60] E. W. Blanch, A. F. Bell, L. Hecht, L. A. Day, L. D. Barron. *J. Mol. Biol.* **1999** ; *290* , 1.
[61] E. W. Blanch, L. Hecht, C. D. Syme, V. Volpetti, G. P. Lomonossoff, K. Nielsen, L. D. Barron. *J. Gen. Virol.* **2002** ; *83* , 2593.
[62] J. Kessler, J. Kapitán, P. Bouř. *J. Phys. Chem. Lett.* **2015** ; *6* , 3314.
[63] I. H. McColl, E. W. Blanch, A. C. Gill, A. G. O. Rhie, M. A. Ritchie, L. Hecht, K. Nielsen, L. D. Barron. *J. Am. Chem. Soc.* **2003** ; *125* , 10019.
[64] F. T. Outeiro, S. Lindquist. *Science* **2003** ; *302* , 1772.
[65] E. J. Jo, N. Fuller, R. P. Rand, P. St George-Hyslop, P. E. Fraser. *J. Mol. Biol.* **2002** ; *315* , 799.
[66] M. F. Ahmad, T. Ramakrishna, B. Raman, C. M. Rao. *J. Mol. Biol.* **2006** ; *364* , 1061.
[67] V. N. Uversky, E. M. Cooper, K. S. Bower, J. Li, A. L. Fink. *FEBS Lett.* **2002** ; *515* , 99.
[68] T. Weymuth, M. Reiher. *J. Phys. Chem. B* **2013** ; *117* , 11943.
[69] E. W. Blanch, L. A. Morozova-Roche, L. Hecht, W. Noppe, L. D. Barron. *Biopolymers* **2000** ; *57* , 235.
[70] S. Yamamoto, H. Watarai. *Chirality* **2012** ; *24* , 97.
[71] M. Junker, P. L. Clark. *Proteins Struct. Funct. Bioinforma.* **2010** ; *78* , 812.